

A Programmable Multifunctional 3D Cancer Cell Invasion Micro Platform

Qian Liu,* Aswin Muralidharan, Abtin Saateh, Zhaoying Ding, Peter ten Dijke, and Pouyan E. Boukany*

In the research of cancer cell invasion and metastasis, recreation of physiologically relevant and faithful three-dimensional (3D) tumor models that recapitulate spatial architecture, spatiotemporal control of cell communication and signaling pathways, and integration of extracellular cues remains an open challenge. Here, a programmable multifunctional 3D cancer cell invasion microbuckets-hydrogel (Mb-H) platform is developed by integrating various function-variable microbuckets and extracellular matrix (ECM)-like hydrogels. Based on this Mb-H micro platform, the aggregation of multi-cancer cells is well controlled to form cancer cell spheroids, and the guiding relationship of single-cell migration and collective cell migration during the epithelial-mesenchymal transition (EMT) of cancer cell invasion are demonstrated. By programming and precisely assembling multiple functions in one system, the Mb-H platform with spatial-temporal controlled release of cytokine transforming growth factor beta (TGF- β) and various functionalized Mb-H platforms with intelligent adjustment of cell-matrix interactions are engineered to coordinate the 3D invasive migration of cancer cell spheroids. This programmable and adaptable 3D cancer cell invasion micro platform takes a new step toward mimicking the dynamically changing (localized) tumor microenvironment and exhibits wide potential applications in cancer research, bio-fabrication, cell signaling, and drug screening.

1. Introduction

Metastasis of tumors is regarded as the largest contributor to cancer-related deaths.^[1] In metastasis, the invasion of cancer cells from the primary tumor through the extracellular matrix (ECM) of the stroma is a crucial step and governed by a multitude of biochemical and biophysical cues, such as cytokines, growth factors, and ECM.^[2] To simplify the complex microenvironmental cues and identify the affecting factors of cancer cell invasion, various 2D monolayer cell migration models have been implemented in *in vitro* matrices, including confined spaces,^[3] nano/micropatterns,^[4] and synthetic fibrous matrices.^[5] Although some independent biochemical and biophysical cell–cell and cell–matrix interactions, and their basic involvement in the invasive migration of cancer cells have been delineated,^[6] due to the dynamic complexity and heterogeneity of solid tumors, identification of the dominant and compensation mechanisms during cancer cell invasion remains

challenging.^[7]


To establish physiologically relevant tumor models, cancer cell spheroids of 3D multicellular aggregates have emerged as a utilizable *in vitro* model. They offer considerable promise, due to the features of spatial architecture, multiple cell–cell and cell–matrix interactions, secretion of soluble mediators, concentration gradients of extracellular cues, and controlled genetic changes.^[8] For 3D cancer cell motility experimental models, the cancer cell spheroids can be coordinated with a scaffold; this can emulate certain advantageous features of natural ECM, like hydrogels that can be tailored with porous networks, high water content, and tunable biochemical and biomechanical properties.^[9] By integrating cancer cell spheroids with engineered hydrogel materials, crucial factors (e.g., stromal components, proteases, and stiffness and microstructures of the matrix) involved in the 3D invasive migration of cancer cells have been profiled.^[2b,10] However, an in-depth research on 3D cancer invasion and metastasis is still limited by the difficulty of mimicking precise spatial organization of spheroids and stroma, dynamic release of cytokines and growth factors, spatiotemporal gradients of functional molecules, and synergy of multiple reactions.

Q. Liu, A. Muralidharan, A. Saateh, P. E. Boukany
Department of Chemical Engineering
Delft University of Technology
van der Maasweg 9, Delft 2629 HZ, The Netherlands
E-mail: liu_qian2@gzlab.ac.cn; p.e.boukany@tudelft.nl

Q. Liu
Guangzhou Laboratory
XingDaoHuanBei Road 9, Guangzhou International Bio Island
Guangzhou, Guangdong Province 510005, P. R. China

Z. Ding
Department of Materials Science and Engineering
Delft University of Technology
Mekelweg 2, Delft 2628 CD, The Netherlands

P. ten Dijke
Department of Cell and Chemical Biology and Oncode Institute
Leiden University Medical Center
Eindhovenweg 20, Leiden 2333 ZC, The Netherlands

 The ORCID identification number(s) for the author(s) of this article can be found under <https://doi.org/10.1002/smll.202107757>.

© 2022 The Authors. Small published by Wiley-VCH GmbH. This is an open access article under the terms of the Creative Commons Attribution-NonCommercial License, which permits use, distribution and reproduction in any medium, provided the original work is properly cited and is not used for commercial purposes.

DOI: 10.1002/smll.202107757

Herein, a programmable multifunctional microbuckets-hydrogel (Mb-H) platform was engineered for studying and managing the 3D invasive migration of cancer cell spheroids. The Mb-H micro platform was fabricated by the assembly of functionalized microbuckets and ECM-like hydrogels to better mimic the complex real tumor microenvironment. In the Mb-H micro platform, cancer cell spheroids were controllably formed in microbuckets and the invasive cell migration in the artificial ECM was demonstrated. Taking the unique advantage of the alterable functionalization on microbuckets, the Mb-H micro platform was further programmed and integrated with multiple functions to establish a more realistic and complex tumor microenvironment. In the functionalized micro platforms, the 3D invasive migration of cancer cell spheroids was able to be manipulated by the directional and dynamical release of the cytokine transforming growth factor (TGF- β) and adjustment of cell–matrix interactions. This versatile and tunable 3D micro platform displays a novel strategy with the synergy of multiple factors in cancer cell invasion and has the potential to recapitulate the complex and heterogeneous tumor microenvironment during metastasis.

2. Construction of 3D Microbuckets-Hydrogel Platform for Cancer Cell Spheroids

The 3D microbuckets-hydrogel (Mb-H) micro platform was constructed by integrating microbuckets with biomimetic hydrogels. Microbuckets were fabricated by asymmetrically crosslinking poly(ethylene glycol) diacrylate of the aqueous two-phase systems in the microfluidic device presented in our previous work (as described in Figure S1, Supporting Information).^[11] A549 lung adenocarcinoma cancer cells were loaded inside the microbuckets (as shown in Figure 1a). After removing the cell culture medium, a hydrogel precursor solution with photoinitiator was added until it completely covered the microbuckets, followed by UV cross-linking to form a 3D Mb-H micro platform. By utilizing the non-cellular adhesive concave microchamber and artificial ECM environment in this Mb-H platform, lung cancer cell spheroids can be formed. As shown in Figures 1b,c, lung cancer cells were trapped inside the microbuckets before and after the gelation of dextran methacrylate (dexMA) hydrogel, and the cells were completely surrounded by the hydrogel, which was labeled with fluorescein isothiocyanate (FITC, cyan color). The percentage of microbuckets occupied by cells was $\approx 87\%$ before adding polymer precursor solution, and slightly decreased to $\approx 78\%$ after the formation of hydrogel due to the removal of cell culture medium (as shown in Figure 1d). Cell viability in the Mb-H micro platform was checked after culturing the cells for 3 days, and it was $\approx 95\%$ (as shown in Figure 1e and Figure S2, Supporting Information). These results indicate that the 3D Mb-H micro platform has been successfully loaded with cancer cells and may provide a potential for research on cancer cell spheroids formation and invasion.

To investigate the formation of cancer cell spheroids, various Mb-H platforms with different hydrogels of dextran methacrylate (dexMA) and gelatin methacrylate (gelMA) were tested. As shown in Figure 1f and Video S1 (Supporting Information),

≈ 10 – 20 lung cancer cells were separately loaded in the microbuckets that were covered with four different hydrogels: 5 wt.% dexMA, 3.5 wt.% dexMA, 5 wt.% gelMA, and 3 wt.% gelMA. Cancer cell spheroids with the size ≈ 100 μm were formed after culturing for 8 days, and their size increased to ≈ 150 μm with the culture time extending to 16 days. The growth curves of cancer cell spheroids in the four different Mb-H platforms were estimated by assuming the cancer cell spheroid as a standard sphere and excluding the disassociated cells. As shown in Figure 1g, spheroids in all systems demonstrated a similar linear growth tendency in the first 10 days. However, with the increase of cell culture time, only the spheroid in the Mb-H platform with 5 wt.% dexMA followed the same linear growth, but spheroids in the platforms containing a lower concentration of dexMA (3.5 wt.%) and gelMA (5 and 3 wt.%) grew faster. This can be attributed to the decrease of hydrogel stiffness from ≈ 40 to ≈ 4 Pa (Figure 1h; Figure S3, Supporting Information) and the increase of average pore size of gel network from ≈ 15 to ≈ 20 μm (Figure 1i; Figure S4, Supporting Information). Of note, the gelMA hydrogel with the intrinsic characteristics of cell adhesive moieties can support the migration of cells, resulting in a relatively large error bar in the corresponding growth curve and a slight decrease of spheroid size in the 3 wt.% gelMA hydrogel. Besides the lung cancer cell spheroids, the formation of MCF7 breast cancer cell spheroids was also amenable in the Mb-H micro platform (Figure S5, Supporting Information). These results indicate that the cancer cell spheroids can be efficiently created in the Mb-H platform, and their proliferation can be well controlled by varying the culture time and hydrogel compositions.

3. Invasive Migration of Cancer Cell Spheroids in the Mb-H Platform

To explore the invasive migration of cancer cell spheroids based on the 3D Mb-H micro platform, transforming growth factor beta (TGF- β) was added to the microenvironment to facilitate cancer cell invasion. A549 VIM RFP cells were used for the real-time monitoring of epithelial-mesenchymal transition (EMT), which is a crucial step during cancer cell metastasis, via the expression of red fluorescent protein (RFP)-tagged vimentin (VIM), a mesenchymal marker. As shown in Figures 2a,b, A549 VIM RFP cells were loaded in the Mb-H micro platforms with different hydrogels of dexMA (5 and 3.5 wt.%) and gelMA (5 and 3 wt.%). After 10 days of culturing, cancer cell spheroids were formed with a stable fluorescence intensity of vimentin (≈ 1 – 1.5 a.u.). However, after adding TGF- β and culturing for 4 days, the fluorescence intensity of vimentin significantly increased to 3–3.8 a.u. ($**p \leq 0.01$, $***p \leq 0.001$, $****p \leq 0.0001$). Meanwhile, the cancer cell spheroids in the Mb-H systems with dexMA hydrogel retained aggregates due to the lack of cellular adhesive moieties, but spheroids in the systems with gelMA hydrogel dissociated and the cells invaded in the hydrogel (Figure S6; Videos S2 and S3, Supporting Information). This indicates that under the condition of TGF- β treatment, the expression of vimentin upregulated, and cancer cells became more invasive in the Mb-H system with gelMA than the system with dexMA due to the intrinsic cellular adhesive property of gelMA. In addition to

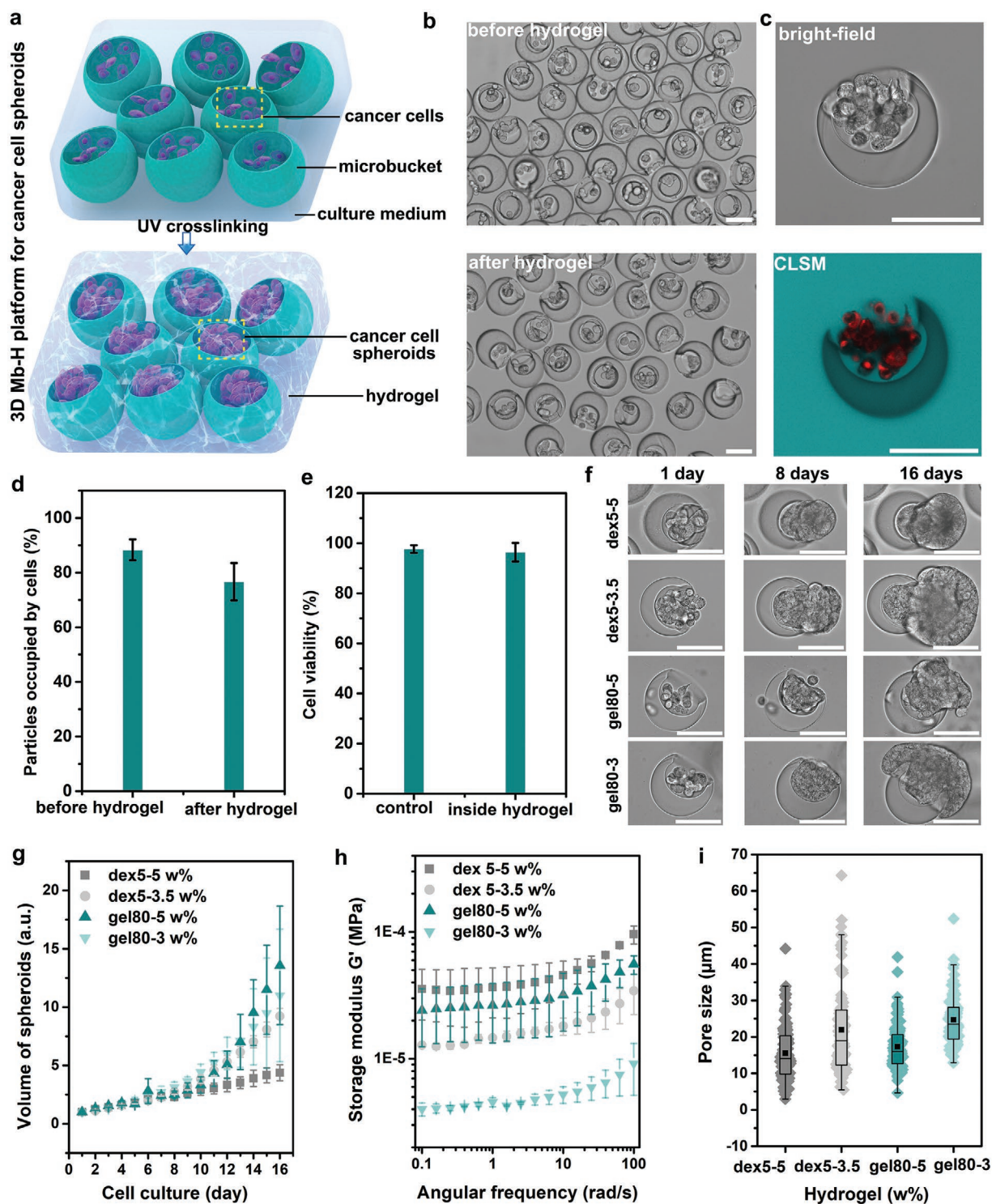


Figure 1. Creating the 3D microbuckets-hydrogel (Mb-H) micro platform for cancer cell spheroids research. a) Schematic illustration of fabrication of the Mb-H system and the formation of cancer cell spheroids. b) Bright-field images of microbuckets loaded with A549 cells before and after covering with dexMA hydrogel. c) Bright-field and confocal laser scanning microscope (CLSM) images of microbucket loaded with A549 cells (red) and covered by dexMA- fluorescein isothiocyanate (FITC) hydrogel (cyan). d) Percentage of microbuckets occupied by A549 cells before and after covering hydrogel. e) Cell viability of A549 cells in the Mb-H platform after culturing for 3 days. Cell-permeant dyes calcein AM and propidium iodide (PI) were used in the live/dead assay. f) Bright-field images of cancer cell spheroids growth in Mb-H micro platforms with different hydrogels of 5 wt.% dexMA, 3.5 wt.% dexMA, 5 wt.% gelMA, and 3 wt.% gelMA, and g) the corresponding growth curves after culturing for 16 days. h) Storage moduli (G' , plotted in the logarithmic scale) of dexMA (5 and 3.5 wt.%) and gelMA (5 and 3 wt.%) hydrogels. i) Pore size distributions of the hydrogels after lyophilization. Scale bar 100 μm .

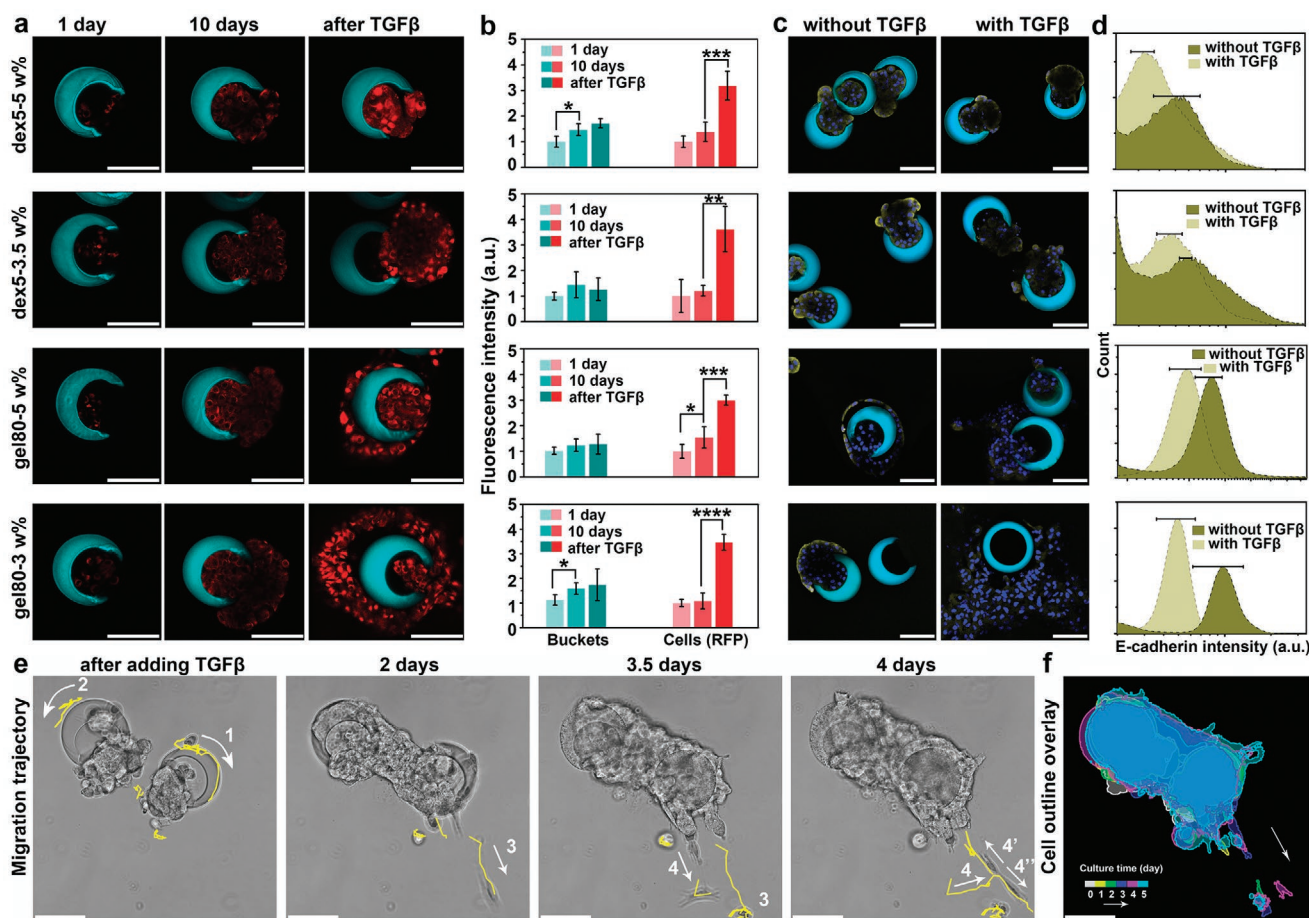


Figure 2. Invasive migration of cancer cells in the Mb-H micro platform with gelMA (3 wt.%). a) CLSM images of A549 VIM RFP cells (red) that are proliferating and migrating in Mb-H platform with different hydrogels before and after adding TGF- β in the cell culture medium and culturing for 4 days. b) Fluorescence intensity of the microbuckets (FITC, cyan) and vimentin (RFP, red) of the cells after 1 day, 10 days, and in the presence of TGF- β . c) Immunofluorescence images of E-cadherin (yellow) in the A549 cell spheroids without and with TGF- β . Cell nuclei were stained by DAPI (blue). d) Intensity distributions of E-cadherin expression in the A549 cell spheroids without and with TGF- β . e) Representative single-cell migration trajectories (yellow line) in 4 days after culturing A549 cell spheroids with TGF- β and the corresponding bright-field images. f) Overlay of cell outlines at different culture times (0–5 days). The concentration of TGF- β in the cell culture medium was 5 ng mL⁻¹. These results are shown as the mean \pm s.d. of three independent experiments, with —three to four buckets per experiment. Lines over bars indicate that conditions were significantly different, as determined by ANOVA with $\alpha = 0.05$ (* $p \leq 0.05$, ** $p \leq 0.01$, *** $p \leq 0.001$, **** $p \leq 0.0001$). Scale bare 100 μ m.

vimentin, another representative biomarker of EMT: Epithelial E-cadherin was also examined by immunofluorescence staining. As shown in Figures 2c,d, the expression of E-cadherin in A549 cells without and with TGF- β was determined by the fluoro-chrome-conjugated secondary antibodies (yellow color). For the cancer cell spheroids in the Mb-H_(dexMA) platform, cancer cells stay clustered and the E-cadherin intensity slightly decreased under the condition of TGF- β treatment. In the Mb-H_(gelMA) platform, the spheroids spread into the hydrogels in the presence of TGF- β , and the E-cadherin expression was downregulated as the intensity shifted to the left. It should be noted that the size of spheroids formed in Mb-H is ≈ 100 – 180μ m, and is well below 500 μ m, above at which a necrotic core is formed. The upregulation of vimentin and downregulation of E-cadherin reveal that EMT can be induced by the addition of TGF- β in the 3D Mb-H micro platform; meanwhile, the invasive migration of cancer cell spheroids is able to be observed in the Mb-H micro platform with gelMA.

The migration trajectory of cancer cell spheroids in response to the TGF- β challenge was further analyzed based on the gelMA-associated Mb-H micro platform. As shown in Figure 2e and Video S4 (Supporting Information), after inducing EMT by adding TGF- β , two single cells (cell 1 and cell 2) migrated along the microbuckets surface and retained connections with the two spheroids. After 2 days, the two spheroids built junctions and merged as a bigger cellular cluster; meanwhile, a single cell with mesenchymal features (cell 3) completely separated from the cellular cluster and migrated. Afterward, the mesenchymal cell 3 stopped migrating and became spherical; in the meantime, mesenchymal cell 4 started migrating individually and leader cells with mesenchymal characteristics formed the tip of the cellular cluster. Subsequently, the mesenchymal cell 4 divided into two cells (4' and 4'') that migrated in opposite directions: cell 4'' migrated away from the cellular cluster, while cell 4' migrated back to the cellular cluster and established a connection with the leader cell at the tip. In addition to the

single mesenchymal cell migration, expansive growth and collective migration of the spheroids were observed by overlapping the cell outlines at different times (Figure 2f). The direction of leader cells in collective migration was consistent with the migrating direction of mesenchymal cells, which is most probably due to the small microtracks generated during the migration of mesenchymal cells.^[12] These results imply that by utilizing the Mb-H micro platform, two modes of 3D invasive migration (including single-cell migration and collective cell migration) during EMT are observed, in the meantime, the relationship between different migrations is demonstrated, that is the single-cell migration provides a direction for the collective cell migration.

4. Guiding 3D Cancer Cell Invasion by a Dynamic TGF- β -Releasing Mb-H Platform

In order to recreate a more realistic tumor microenvironment and guide the 3D invasive migration of cancer cell spheroids during their metastasis, the Mb-H micro platform was designed and equipped with a dynamic release mechanism of growth factors. In vivo, TGF- β , as a multipotential cytokine, is secreted in a latent form in which the TGF- β monomer is noncovalently surrounded and kept in an inactive form by the latency-associated peptide (LAP).^[13] One of the activation mechanisms of the latent TGF- β indicates that the mature bioactive TGF- β dimer can be released through directly digesting the LAP by several proteases (like matrix metalloproteinase (MMP)-2 and MMP-9), which are secreted by most human cancer cells and the associated cells.^[14] Inspired by the biological process, as shown in Figure 3a, a dynamic TGF- β -releasing Mb-H platform has been engineered by modifying the microbuckets with latent TGF- β , followed with dynamically releasing the mature TGF- β via the activation mediated by the cancer cell spheroids.

The latent TGF- β -modified microbuckets were fabricated by binding the biotinylated latent TGF- β to streptavidin-modified microbuckets that were produced based on the selective surface functionalization of hydrogel microparticles in a microfluidic device.^[15] These streptavidin-modified microbuckets provide the potential of being a general principle for functionalizing the buckets with an instructive signal such as latent growth factor. The unmodified and latent TGF- β -modified buckets were loaded with A549 VIM RFP cells and covered with gelMA (3 wt.%) hydrogel. As shown in Figure 3b, cells in the latent TGF- β -modified buckets appeared at the whole surface of the buckets with elongated and invasive shape, and migrated along the surface to the hydrogel around during 8 days of culturing. While cells in the unmodified buckets stayed in the cavity with a round shape and formed spheroids with increasing time (Figure S7, Supporting Information). This implies that the latent TGF- β complex has been immobilized on the microbuckets, and these latent TGF- β -modified microbuckets can perform as TGF- β -releasing microbuckets to induce the invasive migration of cancer cells after being activated.

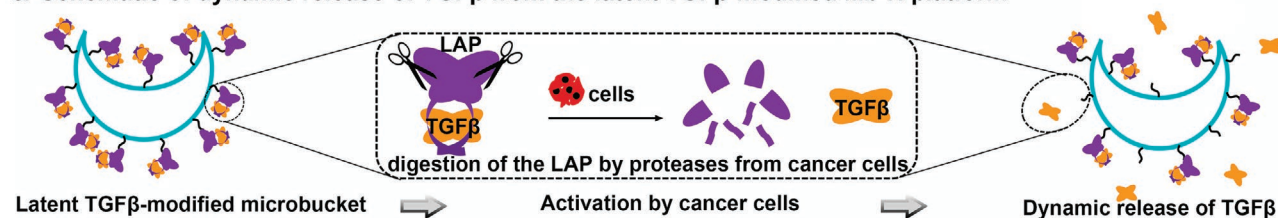
Furthermore, a Mb-H micro platform with the capability of guiding the migration of cancer cell spheroids was programmed by assembling the TGF- β -releasing microbuckets and unmodified microbuckets in one system. As shown in

Figure 3c, an Mb-H micro platform was produced by incorporating gelMA hydrogel with hybrid microbuckets including empty TGF- β -releasing buckets (edges with cyan fluorescence), empty unmodified buckets (homogeneous cyan fluorescence), and unmodified buckets with A549 VIM RFP cell spheroids (homogeneous cyan fluorescence and red fluorescence). At the beginning (0 day), all cells only appeared in the unmodified buckets. However, with the culture time increasing to 8 days, the cells were observed to migrate out of the unmodified buckets and appear on the surface of TGF- β -releasing buckets, implying the release of mature bioactive TGF- β from the latent TGF- β -modified buckets. The 3D images (Figure 3d) show that cells in the unmodified buckets and TGF- β -releasing buckets presented different phenotypes, in which cells in the TGF- β -releasing buckets were more elongated and dispersed than that in the unmodified buckets. In addition, the cancer cells selectively migrated to the TGF- β -releasing buckets, but never to the empty unmodified buckets (Figure 3e), which is most likely due to the chemotactic activity.^[16] The efficient distance to affect the cancer cells, which is defined as the shortest distance between the cancer cell spheroid and the TGF- β -releasing microbucket, was measured below $\approx 65 \mu\text{m}$ in 8 days of culturing (Figure 3f). These results indicate that by integrating the unmodified microbuckets and TGF- β -releasing microbuckets in one system, the functionalized Mb-H micro platform with the directional and dynamic release of TGF- β are constructed, in which the TGF- β -releasing microbuckets act as micro beacons in efficient distance to guide the migrating direction of lung cancer cells during their invasion.

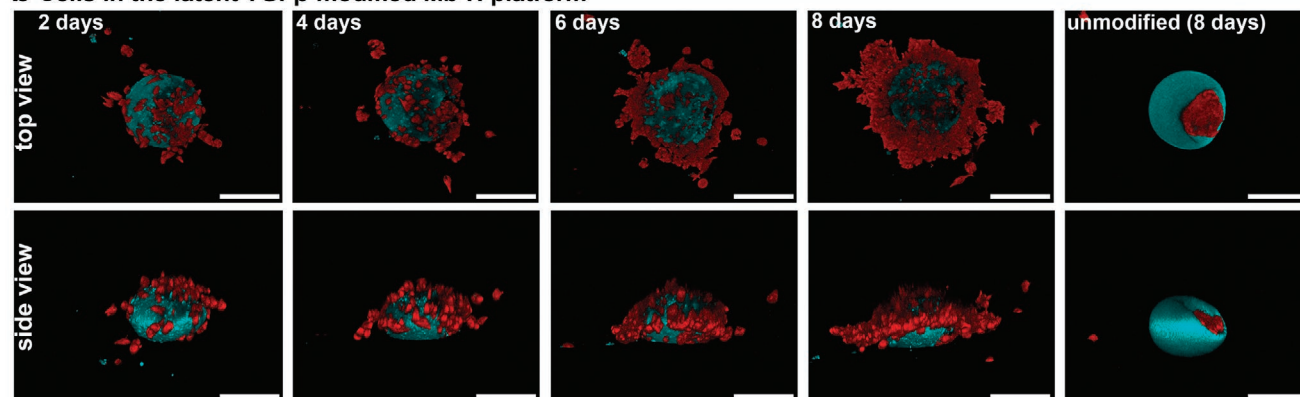
5. Various Functionalized Mb-H Platforms for Adjusting 3D Cancer Cell Invasion

The Mb-H micro platform can be functionalized by assembling versatile microbuckets for different applications on the 3D cancer cell invasion. For instance, the Mb-H micro platform was further functionalized with epithelial cellular adhesion molecule (EpcAM) antibody to enhance the cell–matrix interaction during the invasive migration of cancer cell spheroids (see Figure S8, Supporting Information). As shown in Figure 4a, unmodified and EpcAM antibody-modified microbuckets were separately cultured with A549 VIM RFP cell spheroids. After adding TGF- β and culturing for 4 days, cells from spheroids invasively migrated out of the unmodified buckets and spread in the gelMA hydrogel as usual, however, cells in the EpcAM antibody-modified buckets preferred migrating along with the buckets outer surface with lower invasion to the hydrogel. The distribution of cancer cells during their invasion was represented by the normalized distance from the cell to the geometric center of microbucket (d_c/d_r). As shown in Figure 4b, cells in the unmodified buckets displayed a wide distribution of d_c/d_r from 1 to 5, while a narrow distribution of d_c/d_r from 1 to 1.5 was obtained for the cells in EpcAM antibody-modified buckets. It indicates that the 3D invasive migration of cancer cell spheroids can be adjusted by varying the cell–matrix interaction in the functionalized Mb-H micro platform. In addition, a hybrid Mb-H micro platform with unmodified and EpcAM antibody-modified buckets was constructed to investigate the

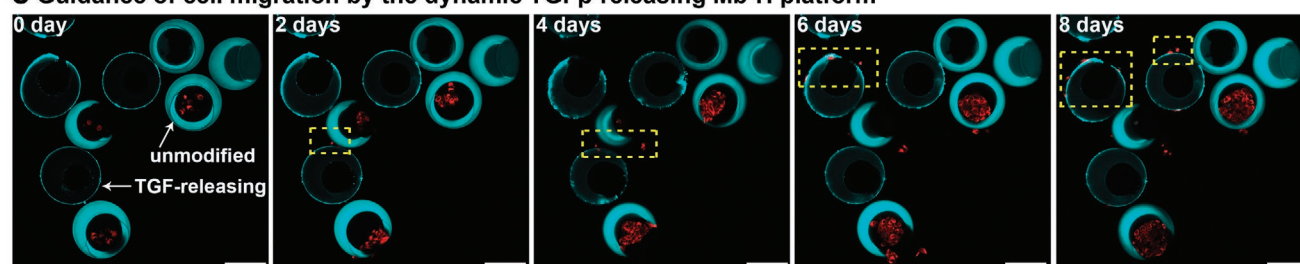
a Schematic of dynamic release of TGF β from the latent TGF β -modified Mb-H platform



b Cells in the latent TGF β -modified Mb-H platform



c Guidance of cell migration by the dynamic TGF β -releasing Mb-H platform



d 3D images

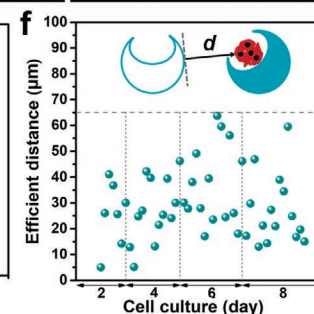
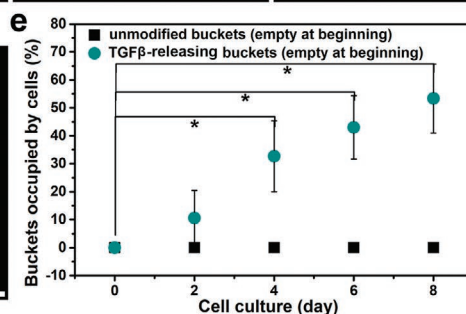
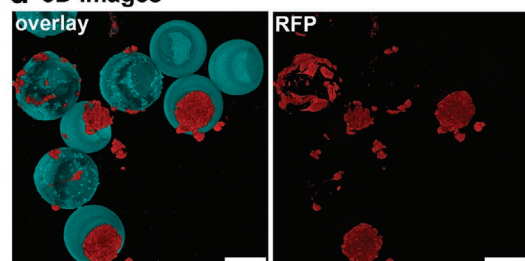


Figure 3. Guidance of cancer cell spheroids invasion by a dynamic TGF- β -releasing Mb-H platform. a) Schematic of dynamic release of bioactive TGF- β dimer from the latent TGF- β -modified bucket after activation by cancer cells. b) Top view (up) and side view (down) of 3D CLSM images of A549 VIM RFP cells in latent TGF- β -modified buckets and unmodified buckets (control). c) Invasive migration of A549 VIM RFP cells in the TGF- β -releasing Mb-H micro platform with latent TGF- β -modified buckets and unmodified buckets. The cells were only loaded in the unmodified buckets at the beginning. d) Overlay and RFP 3D CLSM images of A549 VIM RFP cells in the TGF- β -releasing Mb-H micro platform on the eighth day. e) The percentage of empty microbuckets occupied by cells in the TGF- β -releasing Mb-H micro platform from 0 to 8 days. f) In the TGF- β -releasing Mb-H platform, the efficient distance between the TGF- β -releasing buckets and the cancer cell spheroid in the unmodified buckets (inserted schematic) to guide the cell migration in 8 days. The results are shown as the mean \pm s.d. of three independent experiments, with ≈ 30 buckets ($N_{\text{TGF-modified}} : N_{\text{unmodified}} \approx 3:2$) for each experiment. Scale bare 100 μm . * $p \leq 0.05$ compared to the result of TGF- β -releasing buckets at 0 day.

competition of cell-cell interaction and cell-matrix interaction during the invasion of cancer cell spheroids. As shown in Figure 4c, unmodified and EpCAM antibody-modified microbuckets with lung cancer cell spheroids when embedded in gelMA hydrogel formed the hybrid Mb-H micro platform.

Following the addition of TGF- β , after 2 days, spheroid in the unmodified bucket collectively migrated out of the bucket, whereas spheroid in the EpCAM antibody-modified bucket collectively migrated along the bucket surface resulting from the enhancement of cell-matrix interaction. However, after 4 days,

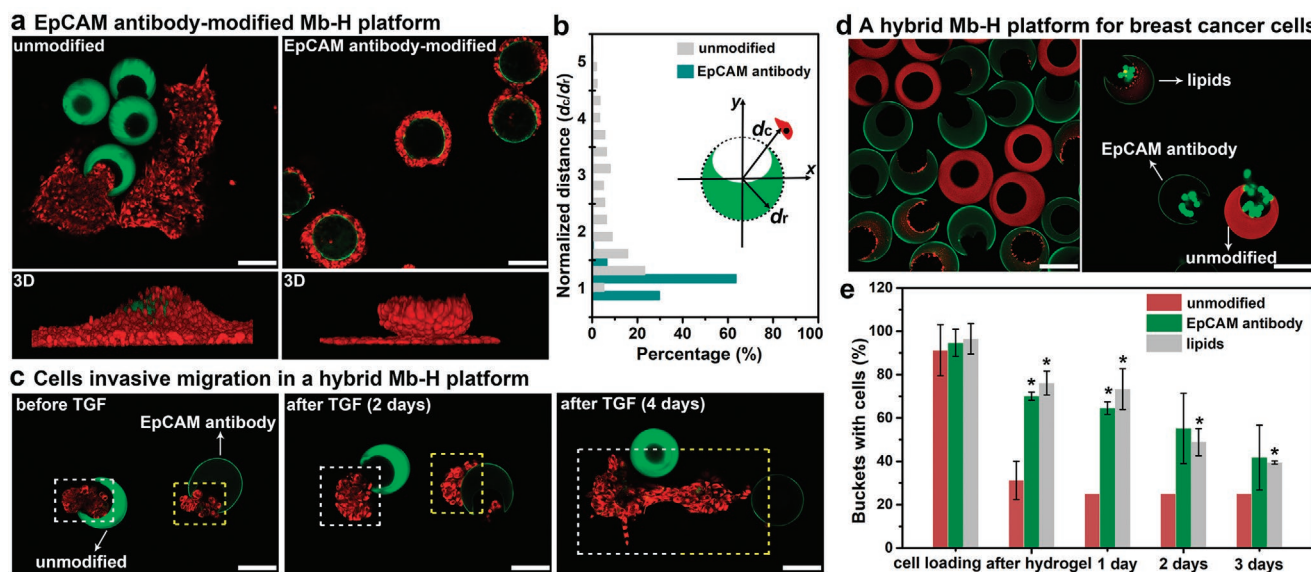


Figure 4. Various functionalized Mb-H micro platforms for adjusting 3D cancer cell invasion. a) CLSM images of the migration of A549 VIM RFP cells in the Mb-H platforms that were respectively embedded with unmodified and EpCAM antibody-modified buckets after being treated with TGF- β (5 ng mL^{-1}) for 4 days. b) The distribution of A549 VIM RFP cells in the Mb-H platforms with unmodified and EpCAM antibody-modified buckets after being treated with TGF- β . The normalized distance was calculated as d_c/d_r (inserted schematic), representing the distance between the center of the circle and the cell (d_c) divided by the radius (d_r). The results are from three independent experiments, with ≈ 20 unmodified buckets and ≈ 20 EpCAM antibody-modified buckets in total. c) CLSM images of the invasive migration of A549 VIM RFP cell spheroids in a hybrid Mb-H_{gelMA} platform with unmodified (green) and EpCAM antibody-modified (green edges) buckets in the presence of TGF- β . d) Breast cancer cells (MDA-MB-231 cells, labeled by calcein AM, green) in a hybrid Mb-H_{gelMA} platform with unmodified (red), proteins (EpCAM antibody, green) and lipids (red, green)-modified buckets. e) Percentage of the functionalized buckets with breast cancer cells after different conditions. These results are shown as the mean \pm s.d. of three independent experiments, with $N_{\text{unmodified}} : N_{\text{EpCAM antibody-modified}} : N_{\text{lipids-modified}} \approx 1:2:2$ for each experiment, $*p \leq 0.05$ compared to the corresponding result of unmodified buckets. Scale bar 100 μm .

these TGF- β -treated cells abandoned the antibody-modified matrix and migrated to the cellular cluster that was from the unmodified bucket, as well as established cell–cell interactions. This reflects that although the cell–matrix interaction can affect the invasive migration of cancer cell spheroids, the cell–cell interaction still plays a major role in guiding the cell invasion.

Not only for the lung cancer cells, a Mb-H micro platform with the assembly of multiple functionalized microbuckets was also exploited to further regulate the invasion of breast cancer cells. To adjust the high motility and invasiveness of the breast cancer cells (MDA-MB-231 cells), unmodified microbuckets and microbuckets with the modification of lipids and proteins were assembled in one gelMA-associated Mb-H micro platform (see Figure S9, Supporting Information). To distinguish the different functionalized microbuckets and research their effects on the breast cancer cells, different fluorescent labels were used on the microbuckets. As shown in Figure 4d, unmodified buckets (red), lipids-modified buckets (red and green edges), and proteins (EpCAM antibody)-modified buckets (green edges) with the breast cancer cells (green) were arranged in one platform. As shown in Figure 4e and Figures S10 and S11 (Supporting Information), the cell occupied rates of different buckets were above 90% after loading breast cancer cells. After being covered with gelMA hydrogel, most cells in the unmodified-buckets left with the buckets occupied rate sharply dropping to 30%, due to the highly migratory nature of MDA-MB-231 cells. However, cells in the lipids and proteins-modified buckets slowly migrated out of the buckets and invaded into the hydrogel, and

the corresponding occupied rates slowly decreased to $\approx 70\%$ and gradually declined to $\approx 45\%$ in the following 3 days of culturing. The postponement of invasive migration of breast cancer cells in the functionalized buckets could be attributed to the variation in surface property of the buckets after introducing proteins and lipids. The latter partially reduces the rejection of MDA-MB-231 cells to the PEG hydrogel buckets. These results demonstrate that the 3D Mb-H micro platform can be programmed and integrated with various functions to target different studies on multiple tumors. It presents the great promise of this 3D Mb-H micro platform for the application in drug screening, and cancer metastasis research.

6. Conclusion

A novel Mb-H micro platform with programmable multi-function was designed and constructed for the 3D invasive migration of cancer cell spheroids based on the combination of microfluidics and soft matter technology. To reproduce the key mechanics of cancer cell metastasis in a real complex tumor microenvironment, microbuckets with variable functions and hydrogels with the features of ECM were combined to establish the Mb-H platform. Based on this Mb-H platform, cancer cells were loaded in the microbuckets and formed cancer cell spheroids with controllable size. The cancer cell spheroids migrated into the hydrogel after facilitating their invasion, accompanying with the epithelial–mesenchymal transition (EMT). Meanwhile,

two modes of 3D invasive migration including single-cell migration and collective cell migration, and the leading behavior of single-cell migration to the collective migration were demonstrated. By programming and assembling multiple functionalized buckets in one platform, various complex and multifunctional Mb-H micro platforms were fabricated. For instance, to further guide the migration of cancer cell spheroids during their invasion, a Mb-H micro platform with the function of directional and dynamic release of TGF- β was engineered based on the activation mechanism of TGF- β (close to the *in vivo* conditions). Furthermore, Mb-H micro platforms with hybrid functions of varying the cell–matrix interaction were displayed to study and adjust the 3D invasive migration of cancer cells. It provides an ingenious strategy for reshaping the dynamic release of growth factors, precise spatiotemporal organization, and synergy of multiple reactions in complex and heterogeneous tumor environments. While the studied spheroids in the Mb-H platform are without a necrotic core, it will be interesting to explore the generation of larger Mb-H platform with spheroids above 400–500 μm .^[19] We anticipate that in that case a necrotic core will be induced promoting a hypoxia-mediated increase in cell invasion, similar to what is observed in poorly vascularized (lung) tumors.

Thus, the established programmable Mb-H platform allows for controllable 3D cancer cell invasion for mechanistic studies by mimicking the desired complexity of the tumor microenvironment. This versatile 3D micro platform exhibits wide potential applications in cancer research, biological engineering, and biomaterials. For instance, the unique platform demonstrated herein has the great potential to be adopted further to co-culturing patient-derived samples (from the tumor, and primary immune cells to patient-derived matrices) and even generate a suitable organoid model for patient specific cancer treatment. In addition, the scalability of our Mb-H platforms provides unique advantages, for high throughput screening applications and performing complex biological assays in a miniaturized manner. The proposed concept opens a new avenue for recreating 3D *in vivo* microenvironment and will inspire more future research in this arena of cancer research and drug screening.

7. Experimental Section

Materials: Poly(ethylene glycol) diacrylate (PEGDA, $M_w = 700$), gelatin methacrylate (gelMA, DS = 80%), dextran ($M_w = 20\,000$), photoinitiator (lithium phenyl-2,4,6-trimethylbenzoylphosphinate), hexadecane, methacryloxyethyl thiocarbonyl rhodamine B, fluorescein methacrylate, fluorescein isothiocyanate-labelled streptavidin (streptavidin-FITC), bovine serum albumin (BSA), and span 80 were purchased from Sigma–Aldrich (Steinheim, Germany). Biotin-PEG-thiol ($M_w = 788$) was purchased from Polypure (Oslo, Norway). Epithelial cellular adhesion molecule (EpCAM) antibody, E-cadherin monoclonal antibody, anti-rabbit IgG (H+L) F(ab')₂ fragment (Alexa fluor 647 conjugate), CellTracker green CMTPX, 4', 6-diamidino-2-phenylindole (DAPI), fetal bovine serum (FBS), Dulbecco's Modified Eagle Medium (DMEM), and Dulbecco's Phosphate Buffered Saline (DPBS) were purchased from Thermo Fisher Scientific Inc. (Landsmeer, Netherlands). Biotinylated human latent TGF- β 1 was purchased from ACROBiosystems Inc (Newark, USA). A549 lung adenocarcinoma cancer cells, MCF7, MDA-MB-231 breast adenocarcinoma cancer cells, and A549 lung adenocarcinoma cancer

cells with red fluorescent protein-tagged vimentin (A549 VIM RFP) were obtained from American Type Culture Collection (ATCC). TGF- β 3 was a kind gift from Dr. A. Hinck, University of Pittsburgh, USA. DexMA ($M_w = 20\,000$, DS = 5%) was synthesized by dextran and glycidyl methacrylate (GMA) as described in the literature.^[17]

Equipment: Axio Observer A1 inverted microscope (Zeiss, 10 \times air objective) with a Zyla 5.5 sCMOS camera (Andor) at 50 frames per second (fps). Mercury-arc light source (HXP 120 V, 120 W) with a band-pass filter 300–400 nm (peak intensity at 365 nm). Andor Inverted Microscope (Zeiss, 10 \times and 20 \times air objectives). Confocal laser scanning microscopy (CLSM, Zeiss LSM 710, 10 \times and 20 \times air objectives and a 40 \times oil immersion objective). Ibidi incubation system. Cell culturing incubation system.

Fabrication of the Mb-H Micro Platform: Microbuckets were generated in the polydimethylsiloxane (PDMS) microfluidic device as reported before.^[11] The microbuckets were placed in a sterile eight-well culture plate. After slowly removing the solution around the microbuckets, 200 μL A549 cell suspension solution with the density $\approx 5 \times 10^4$ cells mL^{-1} (cell culture medium: DMEM with 10% (v/v) FBS and 0.5% (v/v) Anti-Anti) were loaded in the microbuckets, and cultured in the incubator overnight (37 $^\circ\text{C}$ in 5%/95% CO_2 /Air atmosphere). Afterward, microbuckets with cells inside their cavities were carefully pipetted into another well plate, followed by the removal of culture medium. Hydrogel precursor solution with photoinitiator (lithium phenyl-2,4,6-trimethylbenzoylphosphinate, 0.35 w%) was sterilized with a syringe filter (0.22 μm). Two hundred microliters precursor solution was added to the well plate, until completely covered the microbuckets, and treated under UV (365 nm) for 5–10 s to induce gelation and form the Mb-H platform.

Formation of Cancer Cell Spheroids: The Mb-H platform was washed with DPBS (2 times) and culture medium (2 times), then filled with 300 μL culture medium and placed in the incubator for the formation of cancer cell spheroids. The culture medium was changed every 3 days and the growth of spheroids was monitored under a bright-field microscope.

Invasive Migration of Cancer Spheroids: To induce the invasive migration of cancer spheroids, the cell culture medium was removed from the Mb-H micro platform and 300 μL culture medium within TGF- β 3 (5 ng mL^{-1}) was added. The eight-well culture plate was placed in the incubator and checked under the microscope at different times. For the experiment of time series, the eight-well culture plate was placed in an Ibidi incubation system that maintains the cells at 37 $^\circ\text{C}$, 5% CO_2 , and >90% humidity, and tracked under an inverted microscope for 4–6 days.

Functionalization of the Mb-H Micro Platform: The surface of microbuckets were modified with biotin-PEG-SH ($M_w = 788$) and bonded with streptavidin/streptavidin-FITC as reported before.^[15] Afterward, biotinylated human latent TGF- β 1 (50 $\mu\text{g mL}^{-1}$, 200 μL with BSA 0.5% w/v) or biotin conjugated EpCAM antibody (50 $\mu\text{g mL}^{-1}$, 200 μL with BSA 1% w/v and NaN_3 0.09% w/v) was reacted with the streptavidin-modified microbuckets for 48 h, following with washing processes using DPBS (5 times) to remove the unbound molecules. Then the functionalized microbuckets were stored in DPBS for loading cells and covering with dexMA or gelMA hydrogel. The lipids-modified microbuckets were fabricated via a solvent-exchange method.^[18] Details of fabricating the various functionalized microbuckets are described in the Supporting Information.

Statistical Analysis: All data were presented as mean \pm standard deviation (s.d.) of three independent experiments and the statistically significant differences were validated by a one-way analysis of variance (ANOVA) when $\alpha = 0.05$ (* $p \leq 0.05$, ** $p \leq 0.01$, *** $p \leq 0.001$, **** $p \leq 0.0001$).

Supporting Information

Supporting Information is available from the Wiley Online Library or from the author.

Acknowledgements

This work was supported by the European Research Council (ERC) under the European Union's Horizon 2020 research and innovation programme (grant agreement no. 819424). Peter ten Dijke is supported by Cancer Genomics Centre Netherlands (CGC.NL). The authors thank Dr. Da Wei (Institute of Physics, Chinese Academy of Science) for the suggestion to estimate the volume of cancer cell spheroids.

Conflict of Interest

The authors declare no conflict of interest.

Data Availability Statement

The data that support the findings of this study are available from the corresponding author upon reasonable request.

Keywords

3D cancer cell invasion, directional cancer cell migration, dynamic TGF- β release, hydrogels, programmable multiple functions

Received: December 14, 2021

Revised: February 18, 2022

Published online: March 9, 2022

- [1] G. Gundem, P. Van Loo, B. Kremeyer, L. B. Alexandrov, J. M. Tubio, E. Papaemmanuil, D. S. Brewer, H. M. Kallio, G. Högnäs, M. Annala, *Nature* **2015**, 520, 353.
- [2] a) P. Friedl, S. Alexander, *Cell* **2011**, 147, 992; b) N. Peela, D. Truong, H. Saini, H. Chu, S. Mashaghi, S. L. Ham, S. Singh, H. Tavana, B. Mosadegh, M. Nikkhah, *Biomaterials* **2017**, 133, 176.
- [3] a) K. Wilson, A. Lewalle, M. Fritzsche, R. Thorogate, T. Duke, G. Charras, *Nat. Commun.* **2013**, 4, 2896; b) A. Pathak, S. Kumar, *Proc. Natl. Acad. Sci.* **2012**, 109, 10334; c) A. Fink, D. B. Brückner, C. Schreiber, P. J. Röttgermann, C. P. Broedersz, J. O. Rädler, *Biophys. J.* **2020**, 118, 552.
- [4] a) M. Nikkhah, F. Edalat, S. Manoucheri, A. Khademhosseini, *Biomaterials* **2012**, 33, 5230; b) X. Yao, R. Peng, J. Ding, *Adv. Mater.* **2013**, 25, 5257; c) X. Jiang, D. A. Bruzewicz, A. P. Wong, M. Piel, G. M. Whitesides, *Proc. Natl. Acad. Sci.* **2005**, 102, 975; d) D. Garbett, A. Bisaria, C. Yang, D. G. McCarthy, A. Hayer, W. Moerner, T. M. Svitkina, T. Meyer, *Nat. Commun.* **2020**, 11, 4818.
- [5] a) W. Y. Wang, C. D. Davidson, D. Lin, B. M. Baker, *Nat. Commun.* **2019**, 10, 1186; b) J. M. Grolman, P. Weinand, D. J. Mooney, *Proc. Natl. Acad. Sci.* **2020**, 117, 25999; c) K. M. Wisdom, K. Adebowale, J. Chang, J. Y. Lee, S. Nam, R. Desai, N. S. Rossen, M. Rafat, R. B. West, L. Hodgson, *Nat. Commun.* **2018**, 9, 4144; d) W. J. Hadden, J. L. Young, A. W. Holle, M. L. McFetridge, D. Y. Kim, P. Wijesinghe, H. Taylor-Weiner, J. H. Wen, A. R. Lee, K. Bieback, *Proc. Natl. Acad. Sci.* **2017**, 114, 5647.
- [6] a) H. Yamaguchi, J. Condeelis, *Biochim. Biophys. Acta* **2007**, 1773, 642; b) S. V. Plotnikov, A. M. Pasapera, B. Sabass, C. M. Waterman, *Cell* **2012**, 151, 1513; c) G. Charras, E. Sahai, *Nat. Rev. Mol. Cell Biol.* **2014**, 15, 813; d) M. Wang, B. Cheng, Y. Yang, H. Liu, G. Huang, L. Han, F. Li, F. Xu, *Nano Lett.* **2019**, 19, 5949.
- [7] K. M. Yamada, M. Sixt, *Nat. Rev. Mol. Cell Biol.* **2019**, 20, 738.
- [8] a) E. C. Costa, A. F. Moreira, D. de Melo-Diogo, V. M. Gaspar, M. P. Carvalho, I. J. Correia, *Biotechnol. Adv.* **2016**, 34, 1427; b) S. A. Langhans, *Front. Pharmacol.* **2018**, 9, 6.
- [9] a) M. W. Tibbitt, K. S. Anseth, *Biotechnol. Bioeng.* **2009**, 103, 655; b) X. Q. Dou, C. L. Feng, *Adv. Mater.* **2017**, 29, 1604062; c) G. Huang, F. Li, X. Zhao, Y. Ma, Y. Li, M. Lin, G. Jin, T. J. Lu, G. M. Genin, F. Xu, *Chem. Rev.* **2017**, 117, 12764; d) Y. Li, E. Kumacheva, *Sci. Adv.* **2018**, 4, eaas8998.
- [10] a) B. Blanco-Fernandez, V. M. Gaspar, E. Engel, J. F. Mano, *Adv. Sci.* **2021**, 8, 2003129; b) J. Vasudevan, C. T. Lim, J. G. Fernandez, *Adv. Funct. Mater.* **2020**, 30, 2005383; c) N. Peela, F. S. Sam, W. Christenson, D. Truong, A. W. Watson, G. Mounieime, R. Ros, M. Nikkhah, *Biomaterials* **2016**, 81, 72; d) C. Liu, D. L. Mejia, B. Chiang, K. E. Luker, G. D. Luker, *Acta Biomater.* **2018**, 75, 213.
- [11] Q. Liu, M. Zhao, S. Mytnyk, B. Klemm, K. Zhang, Y. Wang, D. Yan, E. Mendes, J. H. van Esch, *Angew. Chem., Int. Ed.* **2019**, 131, 557.
- [12] P. Friedl, K. Wolf, *Cancer Metastasis. Rev.* **2009**, 28, 129.
- [13] a) J. S. Munger, J. G. Harpel, F. G. Giancotti, D. B. Rifkin, *Mol. Biol. Cell* **1998**, 9, 2627; b) M. Shi, J. Zhu, R. Wang, X. Chen, L. Mi, T. Walz, T. A. Springer, *Nature* **2011**, 474, 343.
- [14] a) M. Horiguchi, M. Ota, D. B. Rifkin, *J. Biochem.* **2012**, 152, 321; b) J. Cathcart, A. Pulkoski-Gross, J. Cao, *Genes Dis* **2015**, 2, 26.
- [15] Q. Liu, Z. Yuan, M. Zhao, M. Huisman, G. Drewes, T. Piskorz, S. Mytnyk, G. J. Koper, E. Mendes, J. H. van Esch, *Angew. Chem., Int. Ed.* **2020**, 59, 23748.
- [16] a) S. K. Halder, R. D. Beauchamp, P. K. Datta, *Neoplasia* **2005**, 7, 509. b) T. Ploenes, B. Scholtes, A. Krohn, M. Burger, B. Passlick, J. Müller-Quernheim, G. Zissel, *PLoS One* **2013**, 8, e53068.
- [17] W. N. E. van Dijk-Wolthuis, O. Franssen, H. Talsma, M. J. van Steenberghe, J. J. Kettenes-van den Bosch, W. E. Hennink, *Macromolecules* **1995**, 28, 6317.
- [18] N. Lu, K. Yang, J. Li, Y. Weng, B. Yuan, Y. Ma, *J. Phys. Chem. B* **2013**, 117, 967.
- [19] I. Ziółkowska-Suchanek, *Cells* **2021**, 10, 141.